JOC The Journal of Organic Chemistry

Article

pubs.acs.org/joc

Synthesis, Characterization, and Nanoencapsulation of Tetrathiatriarylmethyl and Tetrachlorotriarylmethyl (Trityl) Radical Derivatives—A Study To Advance Their Applicability as in Vivo EPR Oxygen Sensors

Juliane Frank,[†,§] Marwa Elewa,[†,‡,§] Mohamed M. Said,[‡] Hosam A. El Shihawy,[‡] Mohamed El-Sadek,[∥] Diana Müller,[†] Annette Meister,[⊥] Gerd Hause,[#] Simon Drescher,[†] Hendrik Metz,[†] Peter Imming,*[,†] and Karsten Mäder*[,†]

[†]Institut für Pharmazie, Martin-Luther-Universität (MLU) Halle-Wittenberg, Wolfgang-Langenbeck-Strasse 4, 06120 Halle (Saale), Germany

[‡]Faculty of Pharmacy, Suez Canal University, P.O. 41522, Ismailia, Egypt

[∥]Faculty of Pharmacy, Zagazig University, Zagazig, Egypt

[⊥]Center for Structure and Dynamics of Proteins (MZP), Biocenter Martin-Luther-Universität (MLU) Halle-Wittenberg, Weinbergweg 22, 06120 Halle (Saale), Germany

[#]Biocenter Martin-Luther-Universität (MLU) Halle-Wittenberg, Weinbergweg 22, 06120 Halle (Saale), Germany

Supporting Information

ABSTRACT: Tissue oxygenation plays an important role in the pathophysiology of various diseases and is often a marker of prognosis and therapeutic response. EPR (ESR) is a suitable noninvasive oximetry technique. However, to reliably deploy soluble EPR probes as oxygen sensors in complex biological systems, there is still a need to investigate and improve their specificity, sensitivity, and stability. We reproducibly synthesized various derivatives of tetrathiatriarylmethyl and tetrachlorotriarylmethyl (trityl) radicals. Hydrophilic radicals were investigated in aqueous solution mimicking physiological conditions by, e.g., variation of viscosity and ionic strength. Their specificity was satisfactory, but the oxygen sensitivity was low. To enhance the capability of trityl radicals as oxygen sensors, encapsulation into oily core nanocapsules was performed. Thus, different lipophilic triesters were prepared and characterized in oily solution employing oils typically used in drug formulations, i.e., middle-chain triglycerides and isopropyl myristate. Our screening identified the deuterated ethyl ester of D-TAM (radical **13**) to be suitable. It had an extremely narrow single EPR line under anoxic conditions and excellent oxygen sensitivity. After encapsulation, it retained its oxygen responsiveness and was protected against reduction by ascorbic acid. These biocompatible and highly sensitive nanosensors offer great potential for future EPR oximetry applications in preclinical research.

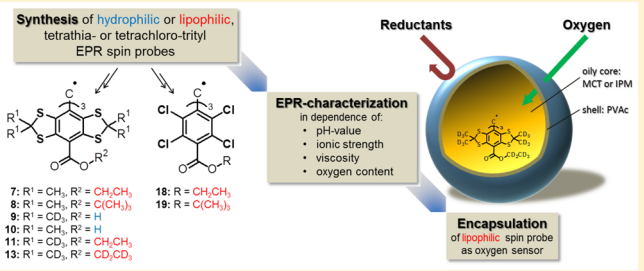

INTRODUCTION

The quantification of oxygen levels in vitro and in vivo is crucial not only for the understanding of physiological processes but also in the assessment and therapy of numerous pathological conditions, such as cancer, peripheral vascular disease, and wounds.[1−3] Various oxygen measurement techniques have been developed, but in vivo oximetry is still challenging. EPR (ESR) oximetry offers several advantages as it enables direct, noninvasive, and repeatable oxygen measurements.[4,5] Spin−spin interactions with the paramagnetic oxygen molecule decrease the relaxation times of EPR spin probe radicals and, therefore, result in a quantifiable broadening of their spectral line width.[6] Two classes of oxygen-sensitive EPR spin probes have been developed. Both have certain advantages and drawbacks. Particulate materials (e.g., carbon-based probes and lithium salts) have attracted much attention as they are very promising oxygen sensors, but they measure oxygen contents only at the implantation site and are often deficient in terms of the reproducibility of their preparation and properties.[7] In contrast, soluble spin probes, e.g., nitroxides and triarylmethyl (trityl, TAM) radicals, are chemically well defined and can distribute evenly within samples.[7] In particular, deuterated trityl radicals and D-,[15]N-substituted nitroxides exhibit favorably narrow single EPR lines.[8,9] However, their oxygen sensitivities are dependent on the solvent, and their signal characteristics are also affected by changes of viscosity and pH value.[10,11] Additionally, when EPR measurements are

Received: April 23, 2015
Published: May 28, 2015

DOI: 10.1021/acs.joc.5b00918
J. Org. Chem. 2015, 80, 6754−6766

conducted in biological systems, the spin probes might lose their signal intensity and their oxygen responsiveness due to interactions with tissues, such as chemical reactions (e.g., reduction or oxidation), protein binding, or fibrous capsule formation.[12,13] With these aspects in mind, we intend to shed more light on EPR oximetry using soluble spin probes, in particular, trityl radicals. Their main limitations might be overcome by appropriate formulations: By encapsulation, their oxygen sensitivities can be improved,[14−17] a defined microenvironment is created, which ensures specificity of the sensors to oxygen, and the capsule shell might provide protection against oxidoreductants[17−19] and prevent biocompatibility concerns.

The first triarylmethyl radical was prepared by Gomberg in 1900.[20] To eliminate hyperfine coupling with hydrogen nuclei and achieve sharp single EPR lines, the phenyl rings were substituted with alkylthio moieties by Nycomed Innovation AB in the 1990s leading to the family of tetrathia-TAM radicals (see Figure 1A).[21,22] Salts of these trityl radicals showed good water solubility as well as stability in the presence of reducing reagents, such as ascorbate and glutathione.[18,23] Another family of trityl radicals, the tetrachloro-TAM radicals, was first introduced in 1967 (see Figure 1B).[24] Upon substitution of the six ortho positions with chlorine atoms, the central methyl carbon was sterically shielded, providing high chemical and thermal stability.[25,26] Tetrachloro-TAM radicals show broader EPR lines due to coupling with the chlorine nuclei in close vicinity but are distinguished by better synthetic accessibility than tetrathia-TAM radicals. Trityl radicals have been employed not only in EPR oximetry[14,27,28] but also in many other applications, e.g., specific detection of superoxide radical anions,[29−31] pH measurements,[32,33] as well as analysis of redox status.[34] Trityl-based spin labels were used for distance measurements, e.g., in nucleic acids.[35] Their long relaxation times made trityl radicals also attractive for (pulsed) EPR imaging[36] and dynamic nuclear polarization (DNP).[37] To achieve intracellular permeability, lipophilic tetrathia-TAM ester derivatives were developed.[38]

In the current work, trityl radicals are studied in order to promote their applicability as EPR oxygen sensors. The study starts with their accessibility, describing reproducible syntheses to obtain various chemically well-defined radicals. Hydrophilic trityls, which can be directly used as molecular oxygen reporters, were investigated in aqueous media mimicking physiological conditions. Lipophilic trityls and pharmaceutical relevant oils were selected for encapsulation to develop biocompatible nanosensors with high oxygen sensitivity, specificity, and stability for in vitro and in vivo EPR oximetry.

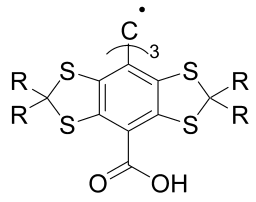

C-TAM: R = CH_3 (radical **10**)
D-TAM: R = CD_3 (radical **9**)
Ox063: R = $(CH_2)_2OH$
Ox031: R = $CH_2O(CH_2)_2OH$

PTMTE: R = $COOCH_2CH_3$ (radical **18**)
PTMTC: R = COOH
PTMTS$^-$-3K$^+$: R = SO_3^- K^+

Figure 1. Chemical structures and common abbreviations of different derivatives of trityl radicals: (A) tetrathia-TAM and (B) tetrachloro-TAM radicals.

RESULTS AND DISCUSSION

Synthesis of Tetrathia-TAM Radicals, Their Deuterated Analogs, and Tetrachloro-TAM Esters. The criteria for trityl radicals that will be useful in pharmaceutical analysis and medical diagnosis are stringent, as detailed in the Introduction. We chose to evaluate the preparation of tetrathia- and tetrachloro-TAM radicals. Both classes and some individual compounds that were of interest to us were known. This is indicated in the Experimental Section. However, trityl radicals are known to be difficult to prepare, and we present herein protocols that worked reproducibly in our hands for known and new derivatives. The synthesis of tetrathia-TAM radicals is shown in Scheme 1.

Scheme 1. Synthesis of Tetrathia-TAM Radicals 7−13[a]

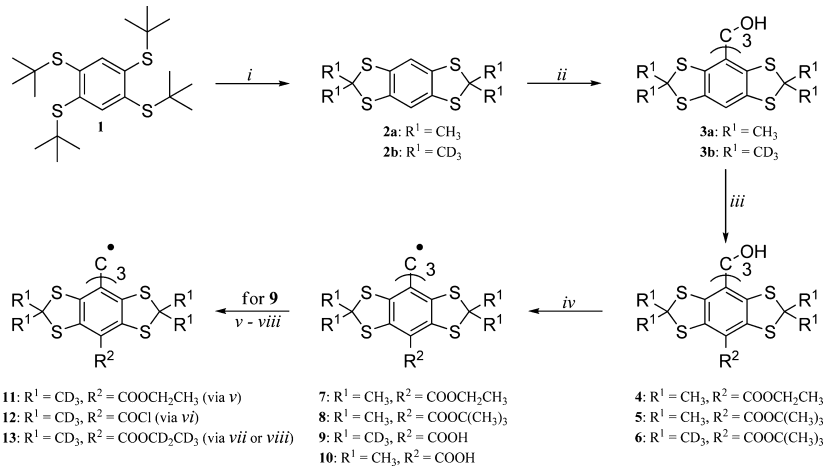

[a]Reagents and conditions: (*i*) HBF_4, acetone or acetone-d_6; (*ii*) *n*-BuLi, methyl chloroformate; (*iii*) *n*-BuLi, TMEDA, and diethyl carbonate or DiBoc; (*iv*) $BF_3 \times Et_2O/SnCl_2$, TFA; (*v*) **9**, TEA, acetonitrile, ethyl chloroformate, DMAP; (*vi*) **9**, $SOCl_2$, TEA; (*vii*) **12**, ethanol-d_6, reflux; (*viii*) **9**, TEA, acetonitrile, ethyl chloroformate-d_5, DMAP.

DOI: 10.1021/acs.joc.5b00918
J. Org. Chem. 2015, 80, 6754−6766

The main hurdle to obtain tetrathia-TAM radicals lies right at the beginning of the synthesis, i.e., the preparation of molar amounts of tetrakis(*tert*-butylthio)benzene (**1**), because of the necessity to use the very odoriferous *tert*-butyl thiol that is added to city gas to detect leakages. We previously published a manageable technique to obtain **1**.[39] The subsequent steps toward the preparation of the tetrathia-TAM radicals shown in Scheme 1 mainly followed published procedures.[9,10,21−23,37,40−42] Modifications regarding the synthetic procedures are detailed in the Experimental Section. Compound **1** was converted into the cyclized arene (**2a**,**b**) by tetrafluoroboric acid (HBF_4) 54% in Et_2O, toluene, and acetone, or acetone-d_6. The triarylmethanols (**3a**,**b**) were prepared by treatment of **2a** or **2b** with *n*-BuLi and the subsequent addition of methyl chloroformate. Reaction of **3a** or **3b** with 10 equiv of *n*-BuLi and tetramethylethylenediamine (TMEDA) resulted in the formation of the corresponding trianion. Different derivatives (compounds **4**−**6**) were prepared through reaction of the appropriate anion with diethyl carbonate (**4**) or di-*tert*-butyldicarbonate (DiBoc) (**5** and **6**). Esters **5** and **6** were subsequently hydrolyzed with trifluoroacetic acid (TFA) overnight at room temperature (RT) to give the tricarboxylic acid (hydrophilic) radicals **9** and **10**. Thin layer chromatography (TLC) of radical **9** revealed the presence of two products: A green spot identified as the target radical **9** and a violet side product identified by MS to be the quinone methide (**20**, see Figure 2) that was recently reported.[41] In contrast to the report and according to MPLC isolation, only 3% of compound **20** had formed. This low amount showed no effect on the line shape of the EPR signal of the trityl radical in solution. Other reports on the preparation of **9** do not mention the formation of **20**. It seems to be formed invariably, its amount increasing on exposure of **9** to light and air.

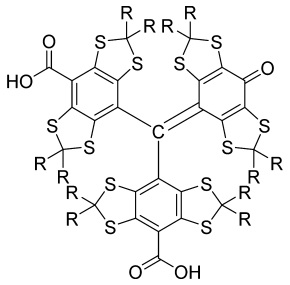

Figure 2. Chemical structure of the quinone methide (**20**)—the product of oxidative decarboxylation reaction of radical **9**.

The conversion of compounds **4** and **5** by boron trifluoride diethyl etherate into the carbocation followed by reduction with stannous chloride gave the lipophilic trityl radicals **7** and **8**.

A mixture of radical **9** and triethylamine (TEA) in acetonitrile was kept at 0 °C. Ethyl chloroformate was added followed by the addition of 4-dimethylaminopyridine (DMAP) to afford the ethyl ester (**11**) in 80% yield. Formation of the fully deuterated ethyl ester analogue **13** was achieved through two methods. Method A involved the esterification of **9** through a two-step reaction: The formation of the corresponding acid chloride **12** with the help of thionyl chloride and TEA followed by reflux with ethanol-d_6 to give radical **13** with 73% yield. Method B included the synthesis of ethyl chloroformate-d_5 and its reaction with a mixture of **9** and TEA followed by addition of DMAP as described before.

The synthesis of tetrachloro-TAM radicals is shown in Scheme 2. Compound **15** was synthesized by Friedel−Crafts alkylation of 1,2,4,5-tetrachlorobenzene (**14**) with $CHCl_3$ in the presence of $AlCl_3$.[43] Reaction of **15** with 10 equiv of *n*-BuLi and TMEDA at low temperature gave the corresponding trianion. Again, a 10-fold excess of the reagent, in this case ethyl chloroformate, had to be used to form compound **16** in 81% yield.[29] Most likely due to the bulkiness of the *tert*-butyl group, not less than 50 equiv of DiBoc was necessary to form compound **17** in an acceptable yield of 49%. Finally, the radicals **18** and **19** were achieved from the corresponding methane derivatives **16** and **17** through reaction with tetrabutylammonium hydroxide and *p*-chloranil in tetrahydrofuran (THF).[44]

Characterization of Hydrophilic Trityl Radicals in Aqueous Solution by EPR Spectroscopy. The line width of soluble EPR spin probes, such as trityl radicals, is directly proportional to the concentration of dissolved oxygen, rendering them suitable for EPR oximetry.[29,45] In this section, we investigate the specificity of hydrophilic trityl radicals for oxygen in aqueous solution which is related with the impact of other environmental parameters, e.g., the viscosity and pH value, on the EPR signal of radical **9**.

Influence of Ionic Strength, Osmolarity, and pH value. The hydrophilic radicals were studied under several conditions to mimic environments in drug formulations or in vivo. Solutions of the radical **9** (c = 50 μM) in phosphate buffer (PB; pH 6.2 and 7.4) as well as phosphate-buffered saline (PBS; pH 6.2 and 7.4) were used to investigate the impact of ionic strength and pH value on EPR line widths under aerated (20.9% O_2) and deoxygenated (~0% O_2) conditions. PBS has ionic strengths and osmolarities which are similar to physiological values, whereas PB has lower ionic strengths/osmolarities. The pH values were chosen to cover the pertinent range occurring in human tissues, namely, 7.0−7.4 in normal tissues and 6.2−7.4 in tumors.[46]

Aerated solutions of compound **9** in the different buffer systems showed similar line widths (ΔB_{PP} = 13.7 ± 0.2 μT) as well as similar EPR line width narrowing (ΔB_{PP} = 3.1 ± 0.1 μT)

Scheme 2. Synthesis of Tetrachloro-TAM Radicals 18 and 19[a]

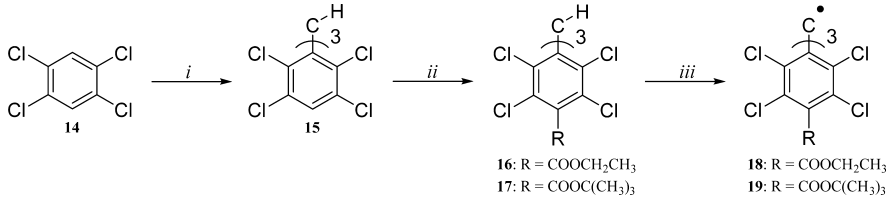

[a]Reagents and conditions: (*i*) $CHCl_3/AlCl_3$; (*ii*) *n*-BuLi, TMEDA, and ethyl chloroformate or DiBoc; (*iii*) Bu_4NOH/*p*-chloranil, THF.

DOI: 10.1021/acs.joc.5b00918
J. Org. Chem. 2015, 80, 6754−6766

after deoxygenation of the samples (Figure 3). The oxygen solubility of aqueous solutions decreases with increasing salt

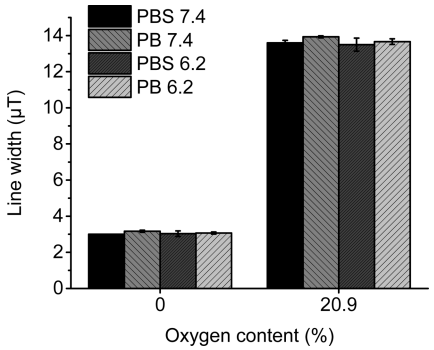

Figure 3. EPR line widths of radical **9** (c = 50 μM) in PB (pH 6.2 and 7.4) and PBS (pH 6.2 and 7.4) under aerated (20.9% O_2) and deoxygenated (~0% O_2) conditions (mean ± SD, n = 3).

content.[47] PBS buffers have a higher ionic strength than PB buffers. However, this difference was not reflected in a change of line width. The pK_a of the undeuterated derivative (radical **10**) was determined to be approximately 4.[10] Thus, at both pH values investigated, the radical should mainly exist in its deprotonated form, without any impact on its EPR properties. In summary, Figure 3 shows that within physiologically relevant limits of ionic strength/osmolarity and pH value, there was a negligible effect of these parameters on the EPR line width of radical **9**.

Impact of Viscosity. To investigate the effect of viscosity on the apparent EPR line width of hydrophilic trityl radicals, radical **9** was dissolved (c = 50 μM) in different glycerol–water mixtures (0–90% glycerol in water, m/m). In absolute glycerol, radical **9** was insoluble. With increasing percentage of glycerol, oxygen solubility and, hence, concentration of dissolved oxygen are decreased.[48] Accordingly, under aerobic conditions, between 0% and 60% (m/m) glycerol content, a decrease in the EPR line width was detected. It was followed by a sharp increase caused by the strong increase of viscosity of the glycerol–water mixtures above 50% (m/m) glycerol content (Figure 4). To support this assumption, the measurements were repeated under deoxygenated conditions. It was found that at up to 40% (m/m) of glycerol, the impact of viscosity on the EPR line width was negligible if compared to the effect of oxygen (see section Oxygen Calibration). A sharp increase in the EPR line width followed, similar to the aerated samples.

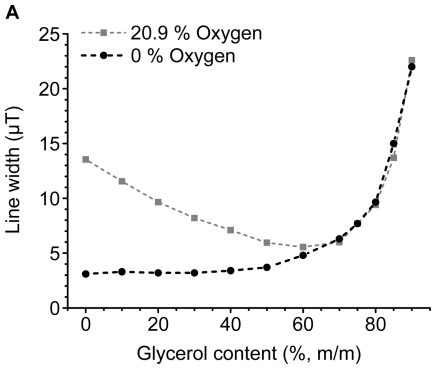

Figure 4. Change in the apparent EPR line width of radical **9** (c = 50 μM) on different glycerol–water mixtures.

Our findings are in agreement with the literature.[11] These results are important with regard to biomedical applications as blood has a dynamic viscosity of η = 3–4 mPa·s at 37 °C,[49] which is only reached at 40% (m/m) of glycerol in water at 20 °C.[50] Thus, provided that there is no specific interaction with biological structures, viscosity by itself should have hardly any effect on EPR line width when using the radicals dissolved in plasma or blood.

EPR Spectroscopic Characterization of Lipophilic Trityl Radicals in Oily Solution. The triesters of the trityl radicals investigated in this work (**7**, **8**, **11**, **13**, **18**, and **19**; see Schemes 1 and 2) proved to be very lipophilic. When these radicals were distributed between octanol and water or middle-chain triglycerides (MCT) and PBS (pH = 7.4) for 2 h at 37 °C, the EPR signal resided in the lipophilic solvent (octanol or MCT) exclusively.

Hence, these trityl radicals were analyzed in oily solution. MCT was chosen because it is generally considered to be biologically inert and already has a long tradition as an ingredient in medicinal products, such as parenteral nutrition nanoemulsions.[51] However, for our purposes, it has a relatively high viscosity of about η = 25–33 mPa·s at 20 °C. As a consequence, the EPR lines are broadened. This may affect the resolution of the EPR spectra and complicate EPR studies. In addition, signal-to-noise ratios are generally lower in highly viscous media since the EPR amplitude is inversely proportional to the square of the line width.[52] As an alternative, the less viscous isopropyl myristate (IPM; η = 5–6 mPa·s at 20 °C) was tested. It is also nontoxic and commonly used, e.g., in topical pharmaceutical formulations.[53]

Solutions of the lipophilic radicals **7**, **8**, **11**, **13**, **18**, and **19** in MCT and IPM (c = 1 mM) were investigated in air (20.9% O_2) and after flushing with nitrogen (~0% O_2). Figure 5 shows the EPR spectra of several trityl radicals in IPM under anoxic conditions. The estimated line widths are listed in Table 1. As predicted from the higher viscosity, the EPR lines under anoxic conditions were broader in MCT. In air, however, the lines were broader in IPM. This is attributed to the higher oxygen solubility and correspondingly higher oxygen content, overruling the effect of viscosity (see next section).

Under anaerobic conditions, the signal of radical **11** displayed superhyperfine coupling with the six equivalent protons of the three methylene groups of the ethyl ester moieties resulting in seven equidistant lines with relative intensities of 1:6:15:20:15:6:1 and a coupling constant of a = 11.3 μT. The coupling pattern was much better resolved in the less viscous IPM. The same ester but with protonated instead of deuterated methyl groups in the ketal moiety (radical **7**) resonated with slightly broader EPR line widths compared to radical **11**. The additional superhyperfine coupling with the protons of the methyl groups affected the signal pattern in deoxygenated solutions (Figure 5). In MCT, only the envelope of the coupling pattern was visible. Deuterium with a nuclear spin of 1, of course, also couples with the electron, but the coupling constant is much smaller compared to the coupling constant of hydrogen.

The *tert*-butyl ester of the nondeuterated trityl (radical **8**) displayed the narrowest single EPR line we observed for the lipophilic esters investigated. As expected, due to the small unresolved hfs with the protons of the *tert*-butyl moieties, the line width in anoxic IPM was slightly broader when compared to the hfs lines of radical **11**. Fully deuterated ethyl ester and methyl ketal groups (radical **13**) also led to exceptionally

DOI: 10.1021/acs.joc.5b00918
J. Org. Chem. 2015, 80, 6754–6766

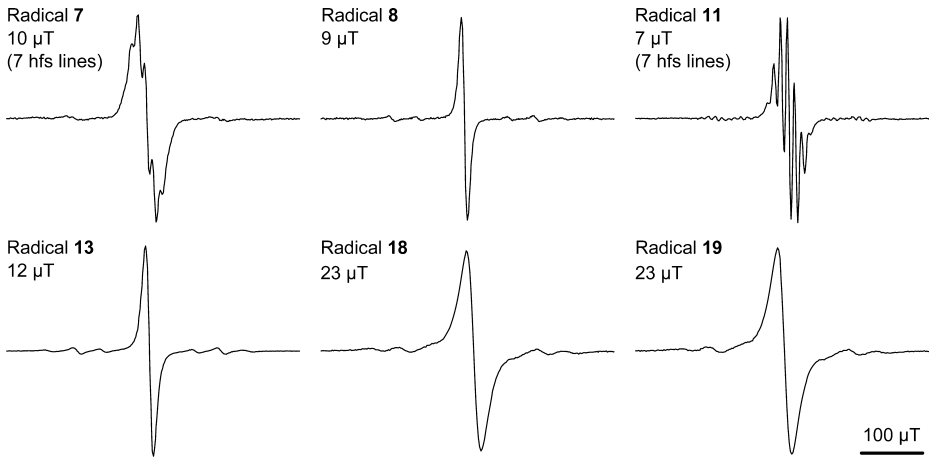

Figure 5. EPR signals of radicals **7**, **8**, **11**, **13**, **18**, and **19** and line widths under anaerobic conditions (~0% O_2) in IPM (c = 1 mM) (hfs = hyperfine splitting). Small side bands caused by hyperfine couplings with ^{13}C were not used in this analysis.

Table 1. EPR Line Widths of Different Lipophilic TAM Triesters Dissolved in MCT and IPM (c = 1 mM) in Air (20.9% O_2) as well as after Flushing with Nitrogen (~0% O_2) and Their Corresponding Oxygen Sensitivities Reported as Mean ± SD (n = 3; n.m. = not measured)

	MCT				IPM			
	EPR line width (μT)		oxygen sensitivity		EPR line width (μT)		oxygen sensitivity	
radical	~0% O_2	20.9% O_2	μT/% O_2	μT/mmHg	~0% O_2	20.9% O_2	μT/% O_2	μT/mmHg
7	15 (7 hfs lines)	57	n.m.	n.m.	10 (7 hfs lines)	94	n.m.	n.m.
8	n.m.	n.m.	n.m.	n.m.	9	88	n.m.	n.m.
11	10 (7 hfs lines)	53	n.m.	n.m.	7 (7 hfs lines)	91	n.m.	n.m.
13	15	44	1.47 ± 0.01	0.20 ± 0.01	12	83	3.59 ± 0.13	0.48 ± 0.02
18	51	82	1.67 ± 0.12	0.23 ± 0.02	23	98	3.83 ± 0.19	0.52 ± 0.03
19	53	90	1.84 ± 0.08	0.25 ± 0.02	23	98	3.75 ± 0.10	0.51 ± 0.02

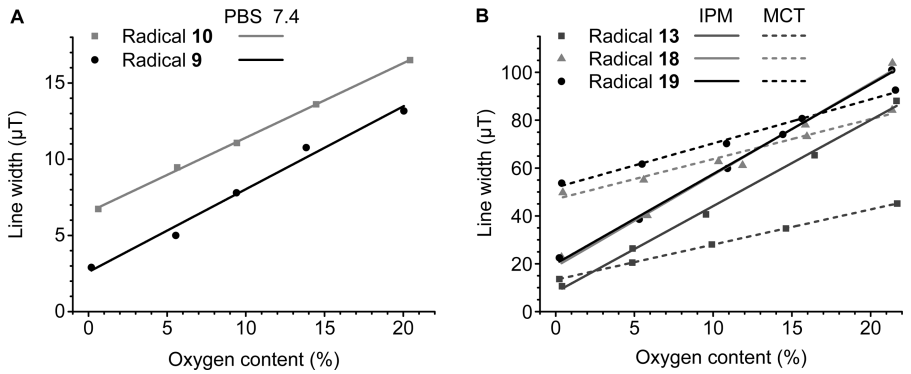

Figure 6. Oxygen calibration curves of (A) hydrophilic trityl radicals in aqueous solution (c = 50 μM) and (B) lipophilic triesters dissolved in MCT and IPM (c = 1 mM) (n = 3).

narrow single lines. Compared to radicals **8** and **11**, the lines were slightly broader in anoxic solutions caused by the unresolved coupling with deuterium nuclei. However, because radical **13** had a better synthetic accessibility than **8**, it was chosen for the following oxygen calibration measurements and encapsulation investigations.

Due to the chlorine splitting, the tetrachloro-TAM triesters generally had broader EPR lines than the tetrathia-TAM derivatives. The *tert*-butyl ester (radical **19**) displayed the same line width as the triethyl ester (radical **18**) in IPM, while in MCT, the line widths were slightly broader. The extremely narrow anoxic line width of **18** and **19** in IPM is remarkable. To our knowledge, only in deoxygenated DMSO (viscosity 2 mPa·s at 20 °C), a line width < 30 μT (namely approximately 28 μT) was reported for tetrachloro-TAM radicals in the literature.[29] Even when dissolved in deoxygenated hexafluorobenzene, the line width of radical **18** was approximately 38 μT, although the viscosity is only 1.2 mPa·s (at 20 °C).

Oxygen Calibration. In this section, the applicability of the selected trityl radicals as oxygen-sensitive spin probes was evaluated. For atmospheric pressure and in vivo applications, only the data between approximately 0% and 20.9% (0–156 mmHg) oxygen are of interest. Solutions of the hydrophilic radicals **9** and **10** (c = 50 μM) in PBS (pH = 7.4) showed a linear relationship between the EPR line width and the oxygen concentration with similar oxygen sensitivities as reported[23,45]

DOI: 10.1021/acs.joc.5b00918
J. Org. Chem. 2015, 80, 6754–6766

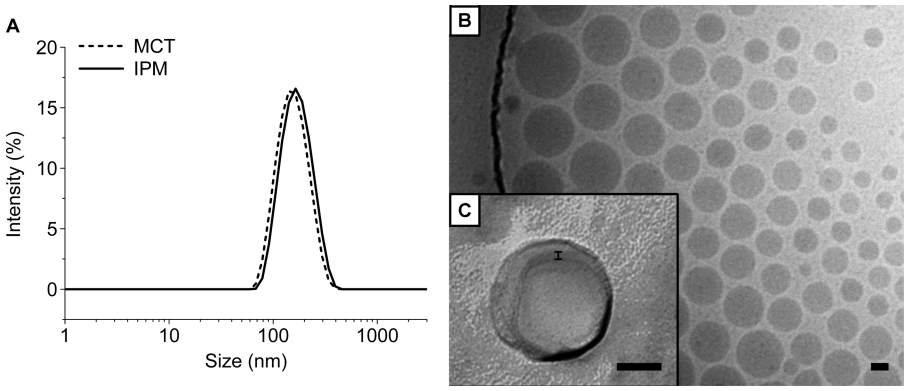

Figure 7. (A) Typical particle size distributions of MCT and IPM NCs. (B) Cryo-TEM image of MCT NCs. (C) Freeze–fracture TEM image of an IPM NC with an estimated shell thickness of about 8 nm (bar size 50 nm).

(Figure 6A). As expected, radical **9** had a narrower line width (ΔB_{PP} = (13.6 ± 0.2) μT at 20.9% O_2) than its undeuterated analogue **10** (ΔB_{PP} = (16.5 ± 0.1) μT at 20.9% O_2). The slope of the curves, i.e., the oxygen sensitivity, was with about 0.5 μT/% O_2 (0.07 μT/mmHg) quite small. As mentioned before, the EPR lines of soluble spin probes are broadened by Heisenberg exchange between the probes and molecular oxygen in solution. According to the Smoluchowski equation, the higher the concentration of dissolved oxygen, the higher the bimolecular collision rate. Due to the low solubility of oxygen in water (the oxygen content in water is only approximately 0.6% (v/v) at 22 °C and 0.213 bar oxygen),[47] the concentration of dissolved oxygen increases only slightly with increasing oxygen partial pressure. Hence, there is only small line broadening, a physicochemical fact affecting any oxygen determination by soluble EPR spin probes in water that is rarely stated.

The oxygen sensitivities of the lipophilic radicals **13**, **18**, and **19** (c = 1 mM) were about 1.7 μT/% O_2 (0.2 μT/mmHg) in MCT and 3.7 μT/% O_2 (0.5 μT/mmHg) in IPM (Figure 6B and Table 1).

Oxygen solubility in oils is generally higher than that in water at a given temperature and pressure,[54] such that the concentration of dissolved oxygen rises noticeably with increasing oxygen partial pressure. Accordingly, the slopes were steeper than in water. By gas chromatography, we determined oxygen contents of 2.2% (v/v) in MCT and 2.9% (v/v) in IPM at 22 °C and 0.213 bar oxygen, both markedly above the oxygen content of water. The different slopes in MCT and IPM were probably caused by the different polarity and especially viscosity of the oils. Remarkably, chemically different radicals, e.g., radicals **13** and **18**, had similar oxygen sensitivities when dissolved in the same solvent. Smaller deviations might be attributed to resolved or unresolved hfs. Thus, obviously, the oxygen sensitivity was rather more affected by the nature of the solvent than the properties of the radical. However, the y intercepts, i.e., line widths under anoxic conditions, were quite different for different radicals as discussed in the previous section.

Of all investigated spin probes and solvents, a solution of radical **13** in IPM was considered best for oxygen measurements: It had the steepest slope with the smallest y intercept. Hence, it combined both excellent oxygen sensitivity and a good signal-to-noise ratio. The high oxygen sensitivity in IPM is comparable with particulate oxygen-sensitive spin probes, such as lithium phthalocyanine (LiPc)[55] or lithium octabutoxynaphthalocyanine (LiNc-BuO),[56] and, thus, very promising for future applications in the field of EPR oximetry as an alternative to particulate materials. For instance, trityl radicals can be employed in lipophilic formulations as it was reported in the literature, e.g., with microspheres,[17] hexafluorobenzene nanoemulsions or solutions,[14,15] or polydimethylsiloxane chips.[16] The present work shows the incorporation into nanocapsules (see next section).

Encapsulation of Trityl Esters and Properties of the Resulting Nanocapsules (NCs). Our studies had shown that to some extent the EPR properties of different water-soluble trityl radicals were independent of their environment, excepting the parameter of interest, viz. oxygen. However, during in vitro or in vivo experiments, conditions can change drastically. Therefore, it was assumed that formulations such as NCs might be a helpful approach. If dissolved in the oily core of NCs, the spin probes are located in a constant microenvironment without being affected by changes of the outer pH value or viscosity. Thereby, NCs can also be used in acidic conditions where hydrophilic trityl radicals would precipitate. Moreover, oxygen molecules can penetrate the capsule shell, turning NCs into oxygen sensors. Since the oxygen solubility in oils is higher than in water, the oxygen sensitivity of the spin probes would be improved by encapsulation (see section above). Highly lipophilic encapsulated probes would stay inside the NCs without being partitioned to the outer aqueous phase, shielding them from oxidoreductants. It is known that suitable formulations are needed to prevent spin probe–tissue interactions in long-term in vivo studies.[12] Thus, not only would the oxygen responsiveness of the spin probes be preserved but also their biocompatibility was improved.

Preparation of the NCs. The nonbiodegradable polymer poly(vinyl acetate) (PVAc), which already had been successfully used as a polymer matrix for particulate spin probes,[57] was chosen for encapsulation of the oily spin probe solutions. NCs with different concentrations (varying from 0.1 to 2%) of PVAc (m/m) and MCT (v/m) in the organic phase were prepared. As a hydrophilic stabilizer, poloxamer 188 (0.25% (m/m) in the aqueous phase) was used, and acetone was used as the organic solvent. In order to obtain the best signal-to-noise ratio of the EPR spectra, the amount of oil inside the NCs needed to be high. On the other hand, the polymer shell surrounding the oily core should be as thin as possible since oxygen has to permeate through the shell. Therefore, NCs should have the lowest possible PVAc and highest possible oil contents. It was found that a concentration of 0.2% (m/m) PVAc and 1.4% (v/m)

DOI: 10.1021/acs.joc.5b00918
J. Org. Chem. 2015, 80, 6754–6766

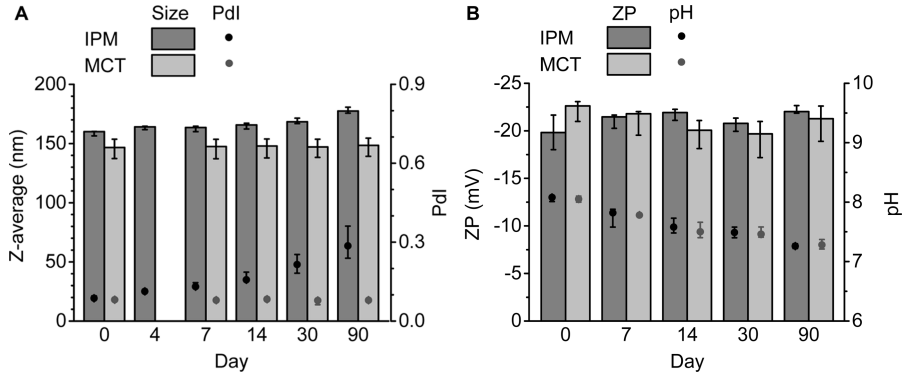

Figure 8. Change in (A) Z-average and PdI of the NCs as well as (B) ZP of the NCs and the pH value of the dispersion on duration of storage at 2−8 °C (n = 3; median and range are shown).

MCT was optimal. In contrast to MCT, it was not possible to obtain stable NCs containing IPM using poloxamer 188. Therefore, other stabilizers were tested, and polysorbate 80 proved to be suitable. The best formulation contained 0.2% (m/m) PVAc and 1.2% IPM (v/m) in the organic phase and 0.2% (m/m) polysorbate 80 in the aqueous phase.

Particle Size, Zeta Potential (ZP), Morphology, and Stability of the NCs. The size of the NCs was determined by photon correlation spectroscopy (PCS). The hydrodynamic diameter (Z-average) typically was about 160 nm for IPM NCs and about 150 nm for MCT NCs. The particle size distributions were monomodal and monodisperse, indicated by a very low polydispersity index (PdI) < 0.1. Figure 7A shows typical particle size distributions of MCT and IPM NCs. The morphology and shell thickness of the NCs were investigated using cryo- and freeze−fracture transmission electron microscopy (TEM). The capsules were spherical in shape; their size varied between approximately 50 and 180 nm (Figure 7B). The deviation from the PCS data might be explained by a particle selection, which usually occurs during sample preparation for cryoTEM. Therefore, the PCS data are considered to represent particle size better. Further, the PVAc shell thickness was determined. Fractured NCs clearly showed a structure with core and shell (Figure 7C). The shell thickness was about 8 nm, very thin, which is in accordance to the literature, where a shell thickness of 10 nm had been found for poly(lactic-co-glycolic acid) (PLGA) NCs.[58] The ZP, as measured in double-distilled water by laser Doppler electrophoresis, was found to be about − 19−22 mV, providing relatively good colloidal stability. However, it must be stated that due to the stabilizers used, the main stabilization mechanism probably was static repulsion. The pH value of the dispersions was about 8, which was in a physiologically well-tolerated range.

In order to examine the stability of the NCs, their size and ZP as well as the pH value of the dispersion were measured not only on the day of preparation but also up to 3 months of storage at 2−8 °C (see Figure 8A and 8B).

Whereas MCT NCs were stable over the whole measurement period, IPM NCs showed instabilities. The Z-average as well as the PdI changed over time of storage. In particular, the increased PdI (from <0.1 to >0.2 after 30 days of storage) indicates aggregation. After 1 week of storage, creaming was observed for the IPM NCs but not for MCT NCs. The reason might be the lower density of IPM with about 850 kg/m^3 compared to MCT with a density of about 950 kg/m^3. The NCs were redispersible by gentle shaking. However, it is assumed that creaming is the reason why IPM NCs tend to aggregate more because of the spatial proximity of the particles. Hence, IPM is less suitable for the preparation of long-term stable NCs. These findings are consistent with the literature.[59] For both oils used, the ZP was stable, whereas the pH value slightly decreased over time, which may have been due to a partial hydrolysis of PVAc and, therefore, release of acetic acid.

Oxygen Calibration of the NCs. The NCs prepared had similar oxygen sensitivities as the unencapsulated solutions (Figure 9). Thus, the encapsulation of the spin probes did not alter their oxygen-sensitive properties. Oxygen obviously diffuses through the polymer shell without any hindrance. The process was reversible (data not shown), meaning that no oxygen was accumulated inside the NCs.

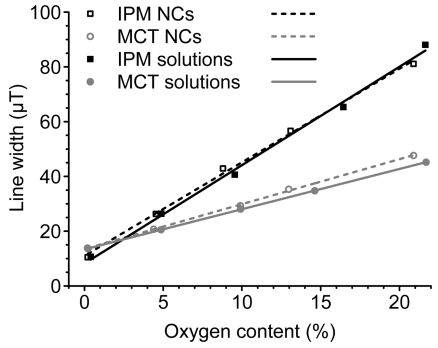

Figure 9. Oxygen calibration curves of oily solutions of radical **13** both incorporated into NCs and unencapsulated. Calculated oxygen sensitivities were 0.46 ± 0.02 (IPM) and 0.22 ± 0.01 μT/mmHg (MCT) for the NCs compared to 0.48 ± 0.02 (IPM) and 0.20 ± 0.01 μT/mmHg (MCT) for the unencapsulated solutions (n = 3).

Ascorbic Acid Reduction Assay. Since the lipophilic triesters (e.g., radical **13**) are uncharged, they may be less protected from reduction by negatively charged reductants since there is no electric repulsion.[18,23] To investigate the stability of encapsulated radicals against reduction, an ascorbic acid reduction assay was carried out. For this, NCs containing solutions of either tempol benzoate (TB) or radical **13** in MCT (c = 1 mM) were prepared. TB is a nitroxide with a log P of approximately 2.[60] It was chosen for comparison because even though it is lipophilic enough for encapsulation, TB is still soluble in water. It is able to partly diffuse through the polymer shell and partition between the two phases. Once outside the NC, it can be reduced by ascorbic acid. Hence, it serves as a positive control.

DOI: 10.1021/acs.joc.5b00918
J. Org. Chem. 2015, 80, 6754−6766

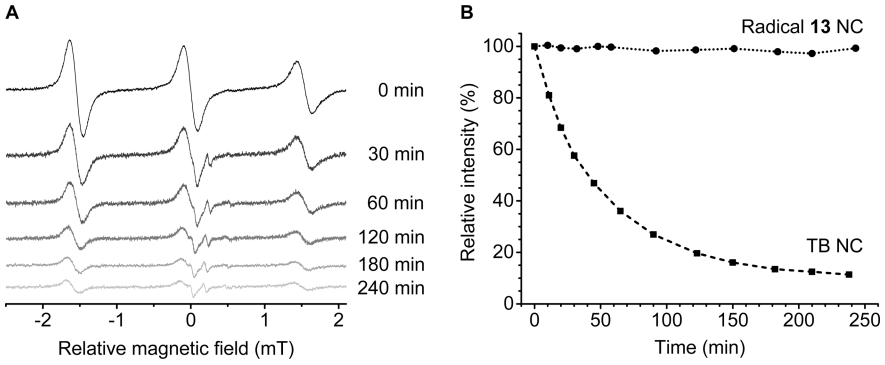

Figure 10. (A) EPR spectra of NCs containing TB during reduction by ascorbic acid. Note that the doublet in the central position arises from ascorbic acid. (B) Change of the EPR signal intensity of NCs with incorporated TB compared to NCs with radical **13**.

As can be seen in Figure 10, TB was reduced by ascorbic acid. The EPR signal intensity decreased to about 11% of the starting value within 240 min. Comparable results had also been found for PLGA NCc.[61] In contrast, radical **13** seemed to stay shielded inside the NCs as it was not reduced by ascorbic acid after 240 min. The result proves that the capsule shell is capable of sterically shielding the incorporated radical from reductants. Moreover, it shows that a very high lipophilicity and correspondingly low water solubility is crucial for effective protection of encapsulated radicals.

CONCLUSION

Reproducible protocols for the synthesis of different derivatives of tetrathia- and tetrachloro-TAM radicals are described. A new readily accessible trityl derivative (radical **13**) with a deuterated core and deuterated ethyl ester groups was devised. The EPR properties of the synthesized radicals were investigated in either aqueous media (hydrophilic radicals) or MCT and IPM (lipophilic triesters). It was shown that within physiological limits of osmolarity, viscosity, and pH value, there was, for practical purposes, no impact on the EPR line widths of the hydrophilic radicals. The nondeuterated lipophilic triethyl esters of C-TAM or D-TAM (radicals **7** and **11**) showed hyperfine splitting in deoxygenated solutions. Other triesters exhibited single EPR lines with line widths directly proportional to the oxygen concentration, rendering them candidates for oxygen measurements. The fully deuterated triethyl ester of D-TAM (radical **13**) had the most promising EPR properties, especially when dissolved in IPM. It had a very narrow EPR line under anoxic conditions and high oxygen sensitivity (~0.5 μT/mmHg). Therefore, solutions of radical **13** in MCT and IPM were encapsulated into NCs. The oxygen responsiveness of the incorporated radical was retained. Using IPM for encapsulation, a high oxygen sensitivity of the NCs could be ensured, especially suitable for measuring low oxygen contents. MCT provided stable NCs for long-term measurements. In addition, despite being uncharged, encapsulated lipophilic trityl radicals were protected against reducing agents such as ascorbic acid. Hydrophilic trityl radicals were shown to be useful EPR oximetry probes, but since the concentration of dissolved oxygen in water does not change much with oxygen partial pressure, lipophilic radicals in oily core NCs led to higher oxygen sensitivity than any water-soluble probe can provide. Encapsulation of lipophilic trityl radicals offers potential for nanosensors with high oxygen sensitivity, specificity, and stability, particularly suitable for EPR oximetry in complex biological systems.

EXPERIMENTAL SECTION

Materials. All chemicals used for synthesis were purchased and used without further purification. Medium-chain triglycerides (Pionier MCT) and isopropyl myristate (Pionier IPM) were purchased from Hansen & Rosenthal KG (Hamburg, Germany), Poloxamer 188 (Lutrol F 68) from BASF SE (Ludwigshafen, Germany), and Polysorbate 80 from Caesar & Loretz GmbH (Hilden, Germany). BASF SE kindly provided poly(vinyl acetate) (PVAc) dispersion 30% (Kollicoat SR 30 D). Water was used in doubly distilled quality.

General Methods for Synthesis. All organic solvents were purified and dried before use and stored over molecular sieves (3 Å). Glassware for reactions under argon atmosphere was oven dried at 100 °C for 2 h prior to use, evacuated, and flushed with argon immediately. The purity of all compounds and the progress of reactions were monitored by thin layer chromatography (TLC) using silica gel 60 F_{254} plates (Merck KGaA, Darmstadt, Germany). Visualizations were accomplished with an UV lamp (254 nm) or iodine staining, and the R_f values given are uncorrected. Purification of the compounds was achieved either by crystallization from appropriate solvents or by flash chromatography. Chemical shifts (δ) are reported in parts per million (ppm) relative to the residual nondeuterated solvent peak in the corresponding spectra (chloroform δ = 7.26, methanol δ = 3.31, DMSO δ = 2.49). The splitting pattern was assigned as follows: s = singlet, bs = broad singlet, d = doublet, t = triplet, q = quartet, m = multiplet; coupling constants (J) are given in Hertz (Hz). ^{13}C NMR chemical shifts were reported as δ values (ppm) relative to the residual nondeuterated solvent peak in the corresponding spectra (chloroform δ = 77.2, methanol δ = 49.0, DMSO δ = 39.5). The samples were analyzed on an orbitrap XL mass spectrometer with a resolving power of 100 000 at m/z 400; samples were introduced to the MS by static nanoelectrospray ionization.

*2,2,6,6-Tetramethylbenzo[1,2-d:4,5-d′]bis[1,3]dithiole (**2a**).*[10,40,42] HBF_4 (54% in Et_2O, 10 mL, 37.0 mmol) was added to a solution of 1,2,4,5-tetra(*tert*-butylthio)benzene (**1**) (16.0 g, 37.2 mmol) in toluene (500 mL). The mixture was stirred for 30 min at RT. Acetone (10 mL, 136 mmol) was added, and the reaction mixture was stirred for 4 h at RT and then heated to reflux overnight. After cooling, a saturated $NaHCO_3$ solution (100 mL) was added carefully, the organic layer was separated, and the aqueous layer was extracted three times with ethyl acetate (EA). The combined organic layers were dried over $MgSO_4$ and concentrated in vacuum. Ethanol (50 mL) was added to the brown solution. The pure product was precipitated and collected by filtration, washed several times with EtOH, and dried to give 7.2 g (68% yield) of white crystals: mp 145−147 °C, R_f = 0.32 (heptane). ^{1}H NMR (400 MHz, $CDCl_3$): δ 7.02 (s, 2H), 1.88 (s, 12H). ^{13}C NMR (100 MHz, $CDCl_3$): δ 135.7, 116.8, 65.7, 31.3. HRMS (ESI): calcd for $C_{12}H_{14}S_4$ $[M]^+$ 285.998; found 285.997.

*2,2,6,6-Tetra(²H₃-methyl)benzo[1,2-d:4,5-d′]bis[1,3]dithiole (**2b**).*[9,21,22] The procedure used for **2a** was applied for the synthesis of **2b** using HBF_4 (54% in Et_2O, 10 mL, 37.0 mmol), compound **1** (16.0 g, 37.2 mmol) in toluene (500 mL), and acetone-d_6 (10 mL, 148 mmol) to afford compound **2b** (7.8 g, 70% yield) as a white solid: mp

DOI: 10.1021/acs.joc.5b00918
J. Org. Chem. 2015, 80, 6754−6766

143−145 °C, R_f = 0.35 (heptane). ^{1}H NMR (400 MHz, $CDCl_3$): δ 7.02 (s, 2H). ^{13}C NMR (100 MHz, $CDCl_3$): δ 135.7, 116.8, 65.7, 31.3. HRMS (ESI): calcd for $C_{12}H_2D_{12}S_4$ $[M]^+$ 298.073; found 298.073.

*Tris[2,2,6,6-tetramethylbenzo[1,2-d:4,5-d′]bis([1,3]dithiole)-4-yl]-methanol (**3a**).*[10,40,42] Compound **2a** (3.5 g, 12.2 mmol) was dissolved in dry diethyl ether (Et_2O) (150 mL) under argon atmosphere. A solution of 2.5 M *n*-BuLi in hexane (4.88 mL, 12.2 mmol) was added dropwise, and the reaction mixture was stirred for 2 h at RT. Methyl chloroformate (0.32 mL, 4.0 mmol) was mixed with Et_2O (40 mL), and the mixture was added slowly with a perfusion pump (flow rate 1 mL/h). Saturated $NaHCO_3$ solution (100 mL) was added, and the reaction mixture was allowed to stir until the formed precipitate completely dissolved. The organic layer was separated, and the aqueous layer was extracted with EA. The combined organic layers were dried over $MgSO_4$, and solvent was evaporated to dryness in a vacuum. The resulting solid was heated at reflux in a mixture of CCl_4 and hexane (1/1, v/v) for 15 min. After cooling, the yellow solid was collected, washed with CCl_4/hexane (1/1, v/v), and dried in a vacuum to give 1.7 g (47% yield) of yellowish solid: mp 250−255 °C, R_f = 0.32 (heptane). ^{1}H NMR (400 MHz, $CDCl_3$): δ 7.17 (s, 3H), 6.20 (s, 1H), 1.82 (s, 9H), 1.80 (s, 9H), 1.72 (s, 9H), 1.68 (s, 9H). ^{13}C NMR (100 MHz, $CDCl_3$): δ 139.2, 138.3, 137.8, 137.2, 131.8, 118.1, 83.6, 64.0, 63.3, 34.8, 32.2, 29.1, 27.6. IR (KBr): ν = 3364, 2954, 2921, 1451, 1147, 756 cm^{-1}. HRMS (ESI): calcd for $C_{37}H_{40}OS_{12}$ $[M]^+$ 883.973; found 883.973.

*Tris[2,2,6,6-($^2H_3$-tetramethyl)benzo[1,2-d:4,5-d′]bis([1,3]dithiole)-4-yl]methanol (**3b**).*[9,21,22] The procedure for the synthesis of **3a** was applied for the synthesis of **3b**. Compound **2b** (3.49 g, 11.7 mmol), *n*-BuLi (4.7 mL, 11.7 mmol), and methyl chloroformate (0.3 mL, 3.9 mmol) in dry Et_2O (150 mL) were used to give **3b** (1.62 g, 45% yield) as a white to yellow solid: mp 250−255 °C, R_f = 0.35 (heptane). ^{1}H NMR (400 MHz, $CDCl_3$): δ 7.17 (s, 3H), 6.21 (s, 1H). ^{13}C NMR (100 MHz, $CDCl_3$): δ 139.5, 138.6, 138.1, 137.6, 132.2, 118.5, 83.9, 63.9, 63.6, 63.2. IR (KBr): ν = 3360, 2953, 2922, 2217, 1374, 1247, 1182, 1003, 861, 754 cm^{-1}. MS (ESI): m/z 943.12 $[M + Na]^+$.

*Tris[8-ethoxycarbonyl-2,2,6,6-tetramethylbenzo[1,2-d:4,5-d′]bis-([1,3]dithiole)-4-yl]methanol (**4**).*[23,40] Compound **3a** (500 mg, 0.57 mmol) and TMEDA (0.85 mL, 5.7 mmol) were mixed in dry *n*-hexane (5 mL) under argon atmosphere and cooled to 0 °C. A solution of 2.5 M *n*-BuLi in hexane (2.3 mL, 5.7 mmol) was added dropwise over 30 min, and the mixture was stirred at RT for 3.5 h. Anhydrous toluene (10 mL) was added, and the reaction mixture was allowed to stir for an additional 1 h and then added slowly via syringe to cold (−25 °C, cooling bath temperature) diethyl carbonate (3.42 mL, 28.3 mmol) diluted with toluene (5 mL). The reaction mixture was allowed to reach RT and stirred overnight. Saturated NaH_2PO_4 solution (10 mL) was added, the organic layer was separated, and the aqueous layer was extracted three times with Et_2O (10 mL). The combined organic layer was washed with water and dried over $MgSO_4$, and the filtrate was passed through a short silica plug. The residue was purified with silica gel, eluting with heptane/EA (9/1) to give 301.4 mg (48% yield) of yellow solid: mp > 280 °C, R_f = 0.4 (heptane/EA, 7/3). ^{1}H NMR (400 MHz, $CDCl_3$): δ 6.77 (s, 1H), 4.50−4.36 (m, 6H), 1.77 (s, 9H), 1.75 (s, 9H), 1.66 (s, 18H), 1.46 (t, J = 7.1 Hz, 9H). ^{13}C NMR (100 MHz, $CDCl_3$): δ 166.2, 141.8, 141.4, 140.3, 139.2, 134.0, 121.3, 84.4, 62.3, 60.9, 60.9, 33.8, 31.9, 29.2, 28.7, 14.3. IR (KBr): ν = 3339, 2975, 1705, 1244, 1221, 1022, 754 cm^{-1}. HRMS (ESI): calcd for $C_{46}H_{52}O_7S_{12}$ $[M]^+$ 1100.035; found 1100.036.

*Tris[8-tert-butoxycarbonyl-2,2,6,6-tetramethylbenzo[1,2-d:4,5-d′]bis([1,3]dithiole)-4-yl]methanol (**5**).*[10,38] Compound **3a** (1.0 g, 1.13 mmol) and TMEDA (1.7 mL, 11.3 mmol) were mixed in dry *n*-hexane (10 mL) under argon atmosphere and cooled to 0 °C. A solution of 2.5 M *n*-BuLi in hexane (4.52 mL, 11.3 mmol) was added dropwise over 30 min, and the mixture was stirred at RT for 3.5 h. Anhydrous toluene (20 mL) was added, and the reaction mixture was allowed to stir for an additional 1 h and then added slowly via syringe to cold (−10 °C, cooling bath temperature) DiBoc (24.66 g, 113 mmol) soaked with toluene (10 mL). The reaction mixture was allowed to reach RT and stirred for 2 days. The reaction was quenched with MeOH (20 mL) added portionwise until no more gas release was observed. The resulting mixture was evaporated, and the thick residue obtained partitioned between aqueous HCl (2 M) and EA. The organic phase was separated, washed with water, and dried over Na_2SO_4. The solvent was evaporated, and the residue was purified with silica gel, eluting with heptane/EA (9/1) to give 522 mg (39% yield) of yellow solid: mp 200−210 °C, R_f = 0.5 (heptane/EA, 7/3). ^{1}H NMR (400 MHz, $CDCl_3$): δ 6.72 (s, 1H), 1.77 (s, 9H), 1.74 (s, 9H), 1.65 (s, 45H). ^{13}C NMR (100 MHz, $CDCl_3$): δ 165.3, 141.2, 140.8, 140.2, 139.1, 133.8, 122.8, 84.2, 60.90, 34.0, 31.9, 29.3, 28.6, 28.4. IR (KBr): ν = 3347, 2977, 2923, 2863, 1698, 1506, 1453, 1365, 1315, 1253, 1220, 1160, 1103, 1011, 845, 755 cm^{-1}. HRMS (ESI): calcd for $C_{52}H_{64}O_7S_{12}$ $[M]^+$ 1184.129; found 1184.131.

*Tris[8-tert-butoxycarbonyl-2,2,6,6-($^2H_3$-tetramethyl)benzo[1,2-d:4,5-d′]bis([1,3]dithiole)-4-yl]methanol (**6**).*[9] The procedure for the synthesis of **5** was applied for the synthesis of **6**. Compound **3b** (1.0 g, 1.08 mmol), TMEDA (1.64 mL, 10.85 mmol), *n*-BuLi (4.34 mL, 10.85 mmol), and DiBoc (23.68 g, 108.5 mmol) were used to give 528 mg (40% yield) of **6** as yellow solid: mp 200−210 °C, R_f = 0.3 (heptane/EA, 5/1). ^{1}H NMR (400 MHz, $CDCl_3$): δ 6.72 (s, 1H), 1.65 (s, 27H). ^{13}C NMR (100 MHz, $CDCl_3$): δ 165.7, 141.5, 141.2, 140.6, 139.4, 134.1, 123.2, 84.5, 60.8, 28.7. IR (KBr): ν = 3351, 2978, 2927, 1701, 1506, 1476, 1455, 1393, 1368, 1314, 1253, 1221, 1161, 1124, 1023, 987, 896, 845 cm^{-1}. MS (ESI): m/z 1243.00 $[M + Na]^+$.

*Tris[8-ethoxycarbonyl-2,2,6,6-tetramethylbenzo[1,2-d:4,5-d′]bis-([1,3]dithiole)-4-yl]methyl Radical (**7**).*[23,42] $BF_3 \times Et_2O$ (73 μL, 0.58 mmol) was added dropwise to a solution of compound **4** (80 mg, 0.073 mmol) in DCM (10 mL) at RT. The mixture was stirred in the dark for 1 h. A solution of $SnCl_2$ (234 mg, 1.23 mmol) dissolved in THF was added to the dark green-blue reaction mixture. The mixture was stirred for 10 min. Saturated KH_2PO_4 solution was added. The organic layer was separated, dried over Na_2SO_4, and concentrated in a vacuum to give 73 mg (92% yield) of the titled radical as a green-brown solid: mp > 280 °C, R_f = 0.4 (heptane/EA, 7/3). IR (KBr): ν = 2957, 2922, 2861, 1703, 1490, 1452, 1365, 1233, 1109, 1043, 792 cm^{-1}. HRMS (ESI): calcd for $C_{46}H_{51}O_6S_{12}$ $[M]^+$ 1083.033; found 1083.034.

*Tris[8-tert-butoxycarbonyl-2,2,6,6-tetramethylbenzo[1,2-d:4,5-d′]bis([1,3]dithiole)-4-yl]methyl Radical (**8**).*[38] The procedure used for the release of radical **7** was applied to release radical **8**. $BF_3 \times Et_2O$ (85 μL, 0.67 mmol), compound **5** (100 mg, 0.084 mmol) in DCM (10 mL), and a solution of $SnCl_2$ (271.81 mg, 1.43 mmol) in THF were used to give 72 mg (73% yield) of the radical **8** as a green solid: mp 200−210 °C, R_f = 0.5 (heptane/EA, 7/3). IR (KBr): ν = 2957, 2923, 1696, 1489, 1454, 1366, 1306, 1280, 1240, 1163, 1135, 1111, 1034, 845 cm^{-1}. HRMS (ESI): calcd. for $C_{52}H_{63}O_6S_{12}$ $[M]^+$ 1167.127; found 1167.126.

*Tris[8-carboxy-2,2,6,6-($^2H_3$-tetramethyl)benzo[1,2-d:4,5-d′]bis-([1,3]dithiole)-4-yl]methyl Radical (**9**).*[9] Compound **6** (100 mg, 82 μmol) was treated with TFA (3 mL) and stirred at RT overnight. The reaction mixture was concentrated and dried to give 82.2 mg (97% yield) as a green-brown solid: mp > 280 °C, R_f = 0.20 ($CHCl_3$/MeOH, 7/3). IR (KBr): ν = 3541−2730, 1666, 1576, 1401, 1345, 1239, 1050 cm^{-1}. HRMS (ESI): calcd for $C_{40}H_3D_{36}O_6S_{12}$ $[M + H]^+$ 1036.173; found 1036.172; calcd for $C_{40}H_3D_{36}O_6S_{12}Na$ $[M + Na]^+$ 1058.155; found 1058.153.

*Tris[8-carboxy-2,2,6,6-tetramethylbenzo[1,2-d:4,5-d′]bis([1,3]-dithiole)-4-yl]methyl Radical (**10**).*[10,40] The procedure used for the synthesis of radical **9** was applied to synthesize radical **10**. Compound **5** (100 mg, 84 μmol) and TFA (3 mL) were reacted to give 79.7 mg (95% yield) as a green-brown solid: mp > 280 °C, R_f = 0.20 ($CHCl_3$/MeOH, 7/3). IR (KBr): ν = 2956, 2921, 1674, 1485, 1451, 1385, 1365, 1226, 1167, 1148, 1111, 866, 725 cm^{-1}. HRMS (ESI): calcd for $C_{40}H_{39}O_6S_{12}$ $[M]^+$ 998.939; found 998.940.

*Tris[8-ethoxy-2,2,6,6-($^2H_3$-tetramethyl)benzo[1,2-d:4,5-d′]bis-([1,3]dithiole)-4-yl]methyl Radical (**11**).*[21,22] Compound **9** (50 mg, 48.3 μmol, 1 equiv) and TEA (7 μL, 48.3 μmol, 1 equiv) were dissolved in acetonitrile (5 mL) under argon atmosphere and cooled to 0 °C. Ethyl chloroformate (0.23 mL, 2.4 mmol, 50 equiv) diluted with acetonitrile (2.5 mL) was added dropwise. The mixture was stirred for further 5 min; then a solution of DMAP (147.5 mg, 1.21

DOI: 10.1021/acs.joc.5b00918
J. Org. Chem. 2015, 80, 6754−6766

mmol, 25 equiv) dissolved in acetonitrile (2 mL) was added. The reaction mixture was allowed to reach RT and stirred overnight. The reaction mixture was concentrated in a vacuum, and the residue was treated with $CHCl_3$ (10 mL) and washed with saturated $NaHCO_3$ solution. The organic layer was separated, washed with HCl (0.1 M, 5 mL) and water (5 mL), dried over $MgSO_4$, and concentrated in a vacuum to give 43 mg (79% yield) of the titled radical as a green-brown solid: mp > 280 °C, R_f = 0.4 (heptane/EA, 7/3). IR (KBr): ν = 3326, 2925, 2850, 1702, 1627, 1575, 1232, 979 cm^{-1}. HRMS (ESI): calcd for $C_{46}H_{15}D_{36}O_6S_{12}$ $[M]^+$ 1119.259; found 1119.259.

*Tris[8-chloro-carbonyl-2,2,6,6-($^2H_3$-tetramethyl)benzo[1,2-d:4,5-d′]bis([1,3]dithiole)-4-yl]methyl Radical (**12**).*[18,40] Compound **9** (150 mg, 0.14 mmol) and dry TEA (121 μL, 0.87 mmol) were dissolved in anhydrous $CHCl_3$ (5 mL), and the mixture was stirred for 10 min at RT. A solution of $SOCl_2$ (105 μL, 1.45 mmol) in $CHCl_3$ (2 mL) was added dropwise over 20 min. The mixture was refluxed for 2.5 h, stirred overnight at RT, and then concentrated to dryness to give a red solid, which was directly used in the next step without further purification: R_f = 0.37 (heptane/EA, 7/3). IR (KBr): ν = 2978, 2945, 2738, 2620, 2602, 2531, 2496, 1699, 1475, 1444, 1398, 1383, 1230, 1172, 1037, 921, 850, 808 cm^{-1}. HRMS (ESI): calcd for $C_{40}D_{36}Cl_3O_3S_{12}$ $[M]^+$ 1091.0605; found 1091.0611.

*Tris[8-($^2H_3$-ethoxy)-2,2,6,6-($^2H_3$-tetramethyl)benzo[1,2-d:4,5-d′]-bis([1,3]dithiole)-4-yl]methyl Radical (**13**).* **Method A:** Compound **12** was dissolved in $CHCl_3$ (5 mL). EtOH-d_6 (0.72 mL, 12.32 mmol) and pyridine (19 μL, 0.24 mmol) were added; the reaction mixture was stirred at 60 °C for 4 h and then at RT overnight. The solvent was evaporated; the residue was dissolved in $CHCl_3$ and washed with water, HCl (0.1 M), and again water three times. The separated organic layer was dried over $MgSO_4$, filtered through a short silica plug, and dried to give 120 mg (73% yield): mp > 280 °C, R_f = 0.40 (heptane/EA, 7/3). MS (ESI): m/z 1158.16 $[M + Na]^+$. IR (KBr): ν = 3337, 2956, 2923, 2717, 2220, 1699, 1489, 1364, 1309, 1280, 1238, 1190, 1139, 1093, 1057, 1022, 980, 791, 753 cm^{-1}. HRMS (ESI): calcd for $C_{46}D_{51}O_6S_{12}$ $[M]^+$ 1134.353; found 1134.355.

Method B: Synthesis of ethyl chloroformate-d_5: To a 2 M solution of phosgene in toluene (5 mL, 9.97 mmol) at 0 °C, pyridine (0.83 mL, 10.31 mmol) was added dropwise and the temperature was kept at 0−5 °C. EtOH-d_6 (0.6 mL, 9.97 mmol) was added dropwise. The reaction mixture was allowed to reach RT, stirred for 2 h, and filtered. The filtrate was used for the next step.[62] The procedure used for the synthesis of radical **11** was applied for the synthesis of radical **13**, method B. Compound **9** (50 mg, 48.3 μmol, 1 equiv), TEA (7 μL, 48.3 μmol, 1 equiv), ethyl chloroformate-d_5 (272.5 mg, 0.24 mL, 2.4 mmol, 50 equiv), and DMAP (147.5 mg, 1.21 mmol, 25 equiv) were used to give 31 mg (56% yield) of the title radical as a green solid. The analytical data of **13** are in accordance with data mentioned above.

*Tris(2,3,5,6-tetrachlorophenyl)methane (**15**).*[43] 1,2,4,5-Tetrachlorobenzene (**14**) (9.6 g, 44 mmol), $AlCl_3$ (0.73 g, 5.2 mol), and $CHCl_3$ (0.4 mL, 4.9 mmol) were mixed in a glass pressure vessel and heated in an oil bath at 160 °C for 45 min. The mixture was then poured onto ice and HCl (1 M, 50 mL) and extracted three times with $CHCl_3$. The organic layer was washed with water and aqueous $NaHCO_3$ and dried over Na_2SO_4. After evaporation, the residue was purified on silica gel, eluting with heptane, to give 1.3 g (40%, based on $CHCl_3$) as white crystals: mp > 280 °C, R_f = 0.67 (heptane). ^1H NMR (400 MHz, $CDCl_3$): δ 7.65 (s, 3H), 6.98 (s, 1H). ^{13}C NMR (100 MHz, $CDCl_3$): δ 138.9, 134.7, 133.9, 133.6, 132.7, 130.7, 56.4. IR (KBr): ν = 3112, 3067, 2926, 1547, 1409, 1387, 1348, 1322, 1235, 1199, 1164, 1099, 975, 866, 844, 782, 759, 704, 690 cm^{-1}. EI-MS: 658 ($C_{19}H_4Cl_{12}$), 621 ($C_{19}H_4Cl_{11}$), 586 ($C_{19}H_4Cl_{10}$), 551 ($C_{19}H_4Cl_9$), 516 ($C_{19}H_4Cl_8$), 479 ($C_{19}H_4Cl_7$), 444 ($C_{19}H_4Cl_6$), 409 ($C_{19}H_4Cl_5$). HRMS (ESI): calcd for $C_{19}H_3Cl_{12}$ $[M - H]^-$ 656.640; found 656.639.

*Tris(4-ethoxycarbonyl-2,3,5,6-tetrachlorophenyl)methane (**16**).*[29] Compound **15** (950 mg, 1.44 mmol) and TMEDA (2.18 mL, 14.44 mmol) were dissolved in dry THF (100 mL) under argon atmosphere and cooled to −78 °C. A solution of 2.5 M *n*-BuLi in hexane (5.8 mL, 14.44 mmol) was added in one portion, and the mixture was stirred at this temperature for 1 h. Ethyl chloroformate (1.37 mL, 14.44 mmol) was added, and the reaction mixture was allowed to reach RT overnight. The solvent was evaporated, and the residue was dissolved in DCM. The organic layer was washed with water and dried over $MgSO_4$. The solvent was evaporated under vacuum, and the residue was purified on silica gel eluting with heptane/EA (12/1) to give 1.0 g (81% yield) of colorless solid: mp 173−175 °C, R_f = 0.26 (heptane/EA, 10/1). ^1H NMR (400 MHz, $CDCl_3$): δ 7.01 (s, 1H), 4.5 (q, J = 7.1 Hz, 6H), 1.42 (t, J = 7.1 Hz, 9H). ^{13}C NMR (100 MHz, $CDCl_3$): δ 163.1, 138.4, 135.5, 135, 134, 130.5, 129.5, 63.1, 56.3, 14. IR (KBr): ν = 2958, 2926, 1744, 1555, 1465, 1445, 1372, 1341, 1329, 1299, 1263, 1225, 1207, 1121, 1095, 1019, 859 cm^{-1}. HRMS (ESI): calcd for $C_{28}H_{17}Cl_{12}O_6$ $[M + H]^+$ 874.720; found 874.719.

*Tris(4-tert-butoxycarbonyl-2,3,5,6-tetrachlorophenyl)methane (**17**).* Compound **15** (500 mg, 0.76 mmol) and TMEDA (1.15 mL, 7.6 mmol) were dissolved in dry THF (50 mL) under argon atmosphere and cooled to −78 °C. A solution of 2.5 M *n*-BuLi in hexane (3 mL, 7.6 mmol) was added in one portion, and the mixture was stirred at this temperature for 1 h. The reaction mixture was added slowly via syringe to DiBoc (8.3 mg, 38 mmol), previously transferred to a dry flask and placed on an ice bath. After the addition was complete, the reaction mixture was allowed to reach RT and stirred for 2 days. The reaction was quenched with MeOH (20 mL) added portionwise until no more gas release was observed. The resulting mixture was evaporated, and the thick residue obtained partitioned between aqueous HCl and $CHCl_3$. The organic phase was separated, washed with water, and dried over $MgSO_4$. The solvent was evaporated, and the residue was purified on silica gel, eluting with heptane/EA (10/1), to give 356.7 mg (49% yield) of a sticky yellow solid: R_f = 0.33 (heptane/EA, 10/1). ^1H NMR (400 MHz, $CDCl_3$): δ 6.99 (s, 1H), 1.62 (s, 27H). ^{13}C NMR (400 MHz, $CDCl_3$): δ 162, 138, 136.2, 134.9, 133.9, 130.2, 129.2, 85.1, 56.2, 27.8. IR (KBr): ν = 2979, 2932, 1736, 1553, 1457, 1394, 1369, 1337, 1274, 1255, 1232, 1157, 1121 cm^{-1}. MS (ESI): m/z 958.82 $[M + H]^+$. HRMS (ESI): calcd for $C_{29}H_{19}Cl_{12}O_4$ $[M - COOC(CH_3)_3]^-$ 856.746; found 856.743.

*Tris(4-ethoxy-carbonyl-2,3,5,6-tetrachlorophenyl)methyl Radical (**18**).*[29] A solution of 1 M Bu_4NOH in MeOH (0.69 mL, 0.69 mmol, 1.2 equiv) was added to a solution of compound **16** (500 mg, 0.57 mmol, 1 equiv) in freshly distilled THF (50 mL) under argon atmosphere. The mixture was stirred in the dark for 1 h. *p*-Chloranil (562.7 mg, 2.29 mmol, 4 equiv) was added as a solid. The mixture was stirred overnight. The solvent was removed, leaving a purple residue, which was purified on silica gel eluting with heptane/EA (4/1) to give 432.8 mg (87% yield) of red solid: mp 158−160 °C, R_f = 0.26 (heptane/EA, 10/1). IR (KBr): ν = 2981, 1742, 1688, 1679, 1572, 1456, 1445, 1373, 1342, 1329, 1260, 1224, 1136, 1111, 1017, 857, 755 cm^{-1}. HRMS (ESI): calcd for $C_{28}H_{15}Cl_{12}O_6$ $[M]^+$ 872.720; found 872.725.

*Tris(4-tert-butoxycarbonyl-2,3,5,6-tetrachlorophenyl)methyl Radical (**19**).*[44] The procedure used for the synthesis of radical **18** was applied for the synthesis of radical **19**. A solution of 1 M Bu_4NOH in methanol (0.25 mL, 0.25 mmol, 1.2 equiv), compound **17** (200 mg, 0.21 mmol, 1 equiv), and *p*-chloranil (205 mg, 0.84 mmol, 4 equiv) were reacted to give 160.7 mg (80% yield) of a red solid: mp 80−83 °C, R_f = 0.33 (heptane/EA, 10/1). IR (KBr): ν = 2980, 2956, 2918, 2850, 1737, 1687, 1573, 1457, 1394, 1370, 1334, 1288, 1240, 1159, 1137, 839, 756 cm^{-1}. HRMS (ESI): calcd for $C_{34}H_{27}Cl_{12}O_6$ $[M]^-$ 956.799; found 956.795.

Sample Preparation for EPR Spectroscopic Characterization. Radical **9** was dissolved (c = 50 μM) in four different buffer systems listed in Table 2.

Additionally, radical **9** was dissolved (c = 50 μM) in mixtures of PBS 7.4 and absolute glycerol, the glycerol content of the mixtures ranging from 0% to 90% (m/m). Radical **10** was dissolved (c = 50 μM) in PBS 7.4. Radicals **13**, **18**, and **19** were dissolved (c = 1 mM) in MCT as well as IPM. All solutions were measured by EPR.

Preparation of NCs. NCs were prepared by interfacial polymer deposition following solvent displacement, a method which is also known as nanoprecipitation and was first described and patented by Fessi et al.[63] First, PVAc was isolated from Kollicoat SR 30 D, which contained about 27% PVAc with a relative molecular mass of about 450 000, 2% povidone, and 0.3% sodium lauryl sulfate. The dispersion

DOI: 10.1021/acs.joc.5b00918
J. Org. Chem. 2015, 80, 6754−6766

Table 2. Buffer Systems Used To Investigate the Impact of Different Ionic Strengths and pH Values on the EPR Line Width of Radical 9

short name	long name	buffer salts	I (mmol/L)	c_{osm} (mosmol/L)	pH
PBS 7.4	phosphate-buffered saline, pH 7.4, Ph.Eur.	Na_2HPO_4, KH_2PO_4, and NaCl	189	327	7.4
PB 7.4	phosphate buffer, 0.02 M, pH 7.4	Na_2HPO_4, KH_2PO_4	49	55	7.4
PBS 6.2	phosphate-buffered saline, pH 6.2	Na_2HPO_4, KH_2PO_4, and NaCl	180	349	6.2
PB 6.2	phosphate buffer, 0.04 M, pH 6.2	Na_2HPO_4, KH_2PO_4	52	86	6.2

was cast onto planar polytetrafluoroethylene (PTFE) coated glass plates. The dried films were washed in doubly distilled water for 5 days in order to remove the water-soluble excipients and finally dried. The resulting PVAc was dissolved in acetone (0.2%, w/w). An oily solution of the EPR spin probe (c = 1 mM) was added to form the organic phase. The organic phase was then injected slowly into an aqueous solution containing either poloxamer 188 or polysorbate 80 under vigorous magnetic stirring. After stirring for at least 10 min, acetone and part of the water were removed by evaporation under reduced pressure at a maximum temperature of 30 °C. The final NCs contained 0.4% (m/m) PVAc and either 2.8% (v/m) MCT and 1% (m/m) poloxamer 188 or 2.4% (v/m) IPM and 0.8% (m/m) polysorbate 80 and were stored at 2−8 °C for further use.

Characterization of the NCs. *Particle Sizes and ZP.* Particle sizes and ZP were measured by PCS, also referred to as dynamic light scattering (DLS), and laser Doppler electrophoresis, respectively, using the Zetasizer Nano ZS (Malvern Instruments GmbH, Herrenberg, Germany). Each sample was diluted 1/25 (v/v) with filtered (pore size 0.22 μm) doubly distilled water, equilibrated at 25 °C, and measured in quintuplicate. The size was measured with 15 runs for 10 s each in the backscattering mode at an angle of 173°; the ZP was measured with 12 runs each and with a delay of 20 s between the runs. The viscosity was assumed to be 0.89 mPa·s. Malvern Zetasizer Software 6.30 was used to obtain Z-averages and PdI by cumulant analysis. The pH value was measured by a glass electrode (Knick Portamess 911(X) pH combined with a pH sensor SE 103, Berlin, Germany). The size, ZP, and pH value of the nanoparticles were measured on the day of preparation as well as up to 3 months after storage.

TEM. TEM was used to investigate the morphology of the NCs. To obtain freeze−fracture images, the samples were freeze fixed 1 day after preparation using a propane jet-freeze device JFD 030 (BAL-TEC, Balzers, Lichtenstein). Thereafter, the samples were freeze−fractured at −150 °C without etching with a freeze−fracture/freeze etching system BAF 060 (BAL-TEC, Balzers, Liechtenstein). The surfaces were shadowed with platinum to produce good topographic contrast (2 nm layer, shadowing angle 45°) and subsequently with carbon to stabilize the ultrathin metal film (20 nm layer, shadowing angle 90°). The replica were floated in sodium chloride (4%, Roth, Karlsruhe, Germany) for 30 min, rinsed in distilled water (10 min), washed in 30% acetone (Roth, Karlsruhe, Germany) for 30 min, and rinsed again in distilled water (10 min). Thereafter, the replica were mounted on copper grids, coated with Formvar film, and observed with a transmission electron microscope (LIBRA 120 PLUS, Carl Zeiss Microscopy GmbH, Oberkochen, Germany) operating at 120 kV. Pictures were taken with a BM-2k-120 Dual-Speed on axis SSCCD-camera (TRS, Moorenweis, Germany). Vitrified specimens for cryo-TEM were prepared by a blotting procedure, performed in a chamber with controlled temperature and humidity using an EM GP grid plunger (LEICA, Wetzlar, Germany). A drop of the sample solution (c = 4 mg PVAc/ml) was placed onto an EM grid coated with a holey carbon film (C-flatTM, Protochips Inc., Raleigh, NC). Excess solution was then removed with a filter paper, leaving a thin film of the solution spanning the holes of the carbon film on the EM grid. Vitrification of the thin film was achieved by rapid plunging of the grid into liquid ethane held just above its freezing point. The vitrified specimens were kept below 108 K during storage, transfers, as well as investigation with the transmission electron microscope (see above). The microscope is equipped with a Gatan 626 cryotransfer system. The obtained electron microscopic images were analyzed using the measureIT software (Olympus Soft Imaging Solutions GmbH, Münster, Germany).

Ascorbic Acid Reduction Assay. The protective properties of the NCs shell against reduction of the incorporated trityl radical were investigated with an ascorbic acid reduction assay based on the one described by Rübe et al.[61] NCs dispersions containing a solution of radical **13** in MCT (c = 1 mM) were concentrated to one-half of the initial volume by evaporation under reduced pressure at a maximum temperature of 30 °C. One part of the dispersions was mixed (1/1, v/v) with PBS 7.4 and the other one with a 2.5 mM solution of ascorbic acid in PBS 7.4. An aliquot of 50 μL each was measured in capillaries using an X-band EPR spectrometer. In the latter case, spectra were recorded for 4 h. Using the MagicPlot software (St. Petersburg, Russia), a first-derivative Lorentzian function was fitted to the recorded line shape and its intensity was calculated as the second integral. The intensity of the spectrum measured in buffer only was defined as the 100% value; all others were calculated relatively. For comparison, NCs containing TB dissolved in MCT (c = 1 mM) were prepared and measured using the same method. In this case, a first-derivative Gaussian function was fitted to the low-field peak and integrated twice to obtain the signal intensity.

Measurements at Defined Oxygen Contents. The samples were flushed with either pure nitrogen or defined mixtures of oxygen and nitrogen at a flow rate of 2 L/min for 3 min using septum vials and cannulae. An anesthesia gas mixer with flow meter tubes (Dräger, Lübeck, Germany) provided defined gas mixtures. The partial pressure of oxygen (in mmHg) in the gas above the solution was confirmed by a needle-type optical oxygen microsensor with temperature control (Type PSt1, PreSens GmbH, Regensburg, Germany) directly after the EPR measurements. Oxygen content (in %) in the gas above the solution was calculated assuming ambient pressure. Oxygen sensitivities were determined by plotting the EPR line widths as a function of the oxygen content and calculating the slope of the linear regression fit.

Oxygen Solubilities. Gas chromatography was used to determine oxygen contents in MCT and IPM. Oils were equilibrated in air at 22 °C. After vacuum extraction, the gas mixtures were passed through a molecular sieve 5 Å packed column using argon as carrier gas in a gas chromatograph with FID, methanizer, and TCD detectors (TOP TOGA GC system with gas extractor, ECH Elektrochemie, Halle, Germany). The area under the curve was determined, and oxygen concentration was calculated by comparing with calibrations obtained from an external standard gas mixture.

EPR Spectroscopy. If not stated otherwise, measurements were conducted in glass vials using an EPR spectrometer at 1.3 GHz (Magnettech, Berlin, Germany) equipped with a re-entrant resonator. Only for the NCs reduction assay, 50 μL of the samples was measured in capillaries using an X-band EPR spectrometer at 9.30−9.55 GHz (Miniscope MS 200, Magnettech, Berlin, Germany). Measurements were conducted under ambient conditions without temperature control. General settings were as follows: microwave power, usually <1 mW; TB NCs, <10 mW; modulation frequency, 100 kHz; sweep, 0.5−2 mT (depending on the line width); TB, 4.7 mT; scan time, 30−3000 s to obtain sufficient signal-to-noise ratios (scan velocity 0.25−25 μT/s). The modulation amplitude was set, such that line distortions were avoided. The MagicPlot software (St. Petersburg, Russia) was used for analysis. In general, a first-derivative Lorentzian function was fitted to the data, and the apparent Lorentzian peak-to-peak line width, i.e., the distance between the maximum and the minimum (ΔB_{PP}), was determined. Line widths < 8 μT were determined by measuring 90° phase shifted. Thereby, the two modulation side bands, having the same line width as the main line, were gathered without the main line. In this case, two Lorentzian functions with a distance of ±3.6 μT from

DOI: 10.1021/acs.joc.5b00918
J. Org. Chem. 2015, 80, 6754−6766

the main line were fitted to the data to extract the line width information. The maximum relative fit error was 2.5%.

■ ASSOCIATED CONTENT

Supporting Information

Proton and carbon NMR spectra of compound **17**. The Supporting Information is available free of charge on the ACS Publications website at DOI: 10.1021/acs.joc.5b00918.

■ AUTHOR INFORMATION

Corresponding Authors

*Phone: +49-345-5525175. Fax: +49-345-5527027. E-mail: peter.imming@pharmazie.uni-halle.de.

*Phone: +49-345-5525167. Fax: +49-345-5527029. E-mail: karsten.maeder@pharmazie.uni-halle.de.

Author Contributions

§J.F. and M.E. contributed equally.

Notes

The authors declare no competing financial interest.

■ ACKNOWLEDGMENTS

We thank Dr. Dieter Stroehl (MLU Halle) for NMR analyses, Dr. Christian Ihling (MLU Halle) for HRMS measurements, Ms. Heike Rudolf (MLU Halle) for IR measurements, Dr. Dorit Wilke (ECH Elektrochemie Halle GmbH) for the determination of oxygen solubilities, and Dr. Sabine Kempe and Dr. Johannes Oidtmann for their contributions to NC preparation. This research was supported by Deutsche Forschungsgemeinschaft (DFG) (MA 1648/8), the Egyptian Ministry of Higher Education and Scientific Research, and the Institut fuer Angewandte Dermatopharmazie (IADP) Halle.

■ REFERENCES

(1) Swartz, H. M.; Khan, N.; Buckey, J.; Comi, R.; Gould, L.; Grinberg, O.; Hartford, A.; Hopf, H.; Hou, H.; Hug, E.; Iwasaki, A.; Lesniewski, P.; Salikhov, I.; Walczak, T. *NMR Biomed.* **2004**, *17*, 335.

(2) Schreml, S.; Szeimies, R. M.; Prantl, L.; Karrer, S.; Landthaler, M.; Babilas, P. *Br. J. Dermatol.* **2010**, *163*, 257.

(3) Walsh, J. C.; Lebedev, A.; Aten, E.; Madsen, K.; Marciano, L.; Kolb, H. C. *Antioxid. Redox Signaling* **2014**, *21*, 1516.

(4) Gallez, B.; Baudelet, C.; Jordan, B. F. *NMR Biomed.* **2004**, *17*, 240.

(5) Khan, N.; Williams, B. B.; Hou, H.; Li, H.; Swartz, H. M. *Antioxid. Redox Signaling* **2007**, *9*, 1169.

(6) Swartz, H. M.; Clarkson, R. B. *Phys. Med. Biol.* **1998**, *43*, 1957.

(7) Ahmad, R.; Kuppusamy, P. *Chem. Rev.* **2010**, *110*, 3212.

(8) Burks, S. R.; Bakhshai, J.; Makowsky, M. A.; Muralidharan, S.; Tsai, P.; Rosen, G. M.; Kao, J. P. Y. *J. Org. Chem.* **2010**, *75*, 6463.

(9) Dhimitruka, I.; Grigorieva, O.; Zweier, J. L.; Khramtsov, V. V. *Bioorg. Med. Chem. Lett.* **2010**, *20*, 3946.

(10) Dhimitruka, I.; Velayutham, M.; Bobko, A. A.; Khramtsov, V. V.; Villamena, F. A.; Hadad, C. M.; Zweier, J. L. *Bioorg. Med. Chem. Lett.* **2007**, *17*, 6801.

(11) Yong, L.; Harbridge, J.; Quine, R. W.; Rinard, G. A.; Eaton, S. S.; Eaton, G. R.; Mailer, C.; Barth, E.; Halpern, H. J. *J. Magn. Reson.* **2001**, *152*, 156.

(12) Gallez, B.; Mäder, K. *Free Radical Biol. Med.* **2000**, *29*, 1078.

(13) Song, Y.; Liu, Y.; Liu, W.; Villamena, F. A.; Zweier, J. L. *RSC Adv.* **2014**, *4*, 47649.

(14) Bratasz, A.; Kulkarni, A. C.; Kuppusamy, P. *Biophys. J.* **2007**, *92*, 2918.

(15) Charlier, N.; Driesschaert, B.; Wauthoz, N.; Beghein, N.; Préat, V.; Amighi, K.; Marchand-Brynaert, J.; Gallez, B. *J. Magn. Reson.* **2009**, *197*, 176.

(16) Meenakshisundaram, G.; Eteshola, E.; Blank, A.; Lee, S. C.; Kuppusamy, P. *Biosens. Bioelectron.* **2010**, *25*, 2283.

(17) Liu, K. J.; Grinstaff, M. W.; Jiang, J.; Suslick, K. S.; Swartz, H. M.; Wang, W. *Biophys. J.* **1994**, *67*, 896.

(18) Liu, Y.; Villamena, F. A.; Zweier, J. L. *Chem. Commun.* **2008**, 4336.

(19) Jagtap, A. P.; Krstic, I.; Kunjir, N. C.; Hänsel, R.; Prisner, T. F.; Sigurdsson, S. T. *Free Radical Res.* **2015**, *49*, 78.

(20) Gomberg, M. *J. Am. Chem. Soc.* **1900**, *22*, 757.

(21) Andersson, S.; Radner, F.; Rydbeek, A.; Servin, R.; Wistrand, L. G. U.S. Patent US 5530140 A 19960625, 1996.

(22) Andersson, S.; Radner, F.; Rydbeck, A.; Servin, R.; Wistrand, L.-G. U.S. Patent US 5728370 A 19980317, 1998.

(23) Xia, S.; Villamena, F. A.; Hadad, C. M.; Kuppusamy, P.; Li, Y.; Zhu, H.; Zweier, J. L. *J. Org. Chem.* **2006**, *71*, 7268.

(24) Ballester, M. *Pure Appl. Chem.* **1967**, *15*, 123.

(25) Ballester, M.; Riera-Figueras, J.; Castaner, J.; Badfa, C.; Monso, J. M. *J. Am. Chem. Soc.* **1971**, *93*, 2215.

(26) Ballester, M.; Riera, J.; Castaner, J.; Rodriguez, A.; Rovira, C.; Veciana, J. *J. Org. Chem.* **1982**, *47*, 4498.

(27) Kutala, V. K.; Parinandi, N. L.; Pandian, R. P.; Kuppusamy, P. *Antioxid. Redox Signaling* **2004**, *6*, 597.

(28) Liu, Y.; Villamena, F. A.; Sun, J.; Wang, T.-y.; Zweier, J. L. *Free Radical Biol. Med.* **2009**, *46*, 876.

(29) Dang, V.; Wang, J.; Feng, S.; Buron, C.; Villamena, F. A.; Wang, P. G.; Kuppusamy, P. *Bioorg. Med. Chem. Lett.* **2007**, *17*, 4062.

(30) Kutala, V. K.; Villamena, F. A.; Ilangovan, G.; Maspoch, D.; Roques, N.; Veciana, J.; Rovira, C.; Kuppusamy, P. *J. Phys. Chem. B* **2008**, *112*, 158.

(31) Liu, Y.; Song, Y.; De Pascali, F.; Liu, X.; Villamena, F. A.; Zweier, J. L. *Free Radical Biol. Med.* **2012**, *53*, 2081.

(32) Bobko, A. A.; Dhimitruka, I.; Zweier, J. L.; Khramtsov, V. V. *J. Am. Chem. Soc.* **2007**, *129*, 7240.

(33) Driesschaert, B.; Marchand, V.; Levêque, P.; Gallez, B.; Marchand-Brynaert, J. *Chem. Commun.* **2012**, *48*, 4049.

(34) Liu, Y.; Villamena, F. A.; Song, Y.; Sun, J.; Rockenbauer, A.; Zweier, J. L. *J. Org. Chem.* **2010**, *75*, 7796.

(35) Shevelev, G. Y.; Krumkacheva, O. A.; Lomzov, A. A.; Kuzhelev, A. A.; Rogozhnikova, O. Y.; Trukhin, D. V.; Troitskaya, T. I.; Tormyshev, V. M.; Fedin, M. V.; Pyshnyi, D. V. *J. Am. Chem. Soc.* **2014**, *136*, 9874.

(36) Bobko, A. A.; Dhimitruka, I.; Zweier, J. L.; Khramtsov, V. V. *Angew. Chem.* **2014**, *126*, 2773.

(37) Karlsson, M.; Napolitano, R.; Visigalli, M.; Lerche, M. H.; Jensen, P. R.; Tedoldi, F. WO Patent WO 2014009240A1 20140116, 2014.

(38) Liu, Y.; Villamena, F. A.; Sun, J.; Xu, Y.; Dhimitruka, I.; Zweier, J. L. *J. Org. Chem.* **2008**, *73*, 1490.

(39) Müller, D.; Adelsberger, K.; Imming, P. *Synth. Commun.* **2013**, *43*, 1447.

(40) Rogozhnikova, O. Y.; Vasiliev, V. G.; Troitskaya, T. I.; Trukhin, D. V.; Mikhalina, T. V.; Halpern, H. J.; Tormyshev, V. M. *Eur. J. Org. Chem.* **2013**, 3347.

(41) Tormyshev, V. M.; Genaev, A. M.; Salnikov, G. E.; Rogozhnikova, O. Y.; Troitskaya, T. I.; Trukhin, D. V.; Mamatyuk, V. I.; Fadeev, D. S.; Halpern, H. J. *Eur. J. Org. Chem.* **2012**, 623.

(42) Reddy, T. J.; Iwama, T.; Halpern, H. J.; Rawal, V. H. *J. Org. Chem.* **2002**, *67*, 4635.

(43) Ballester, M.; Riera, J.; Castañer, J.; Rovira, C.; Armet, O. *Synthesis* **1986**, 64.

(44) Roques, N.; Maspoch, D.; Wurst, K.; Ruiz-Molina, D.; Rovira, C.; Veciana, J. *Chem.—Eur. J.* **2006**, *12*, 9238.

(45) Ardenkjær-Larsen, J. H.; Laursen, I.; Leunbach, I.; Ehnholm, G.; Wistrand, L. G.; Petersson, J. S.; Golman, K. *J. Magn. Reson.* **1998**, *133*, 1.

(46) Vaupel, P.; Kallinowski, F.; Okunieff, P. *Cancer Res.* **1989**, *49*, 6449.

(47) Battino, R.; Rettich, T. R.; Tominaga, T. *J. Phys. Chem. Ref. Data* **1983**, *12*, 163.

DOI: 10.1021/acs.joc.5b00918
J. Org. Chem. 2015, 80, 6754−6766

(48) Kutsche, I.; Gildehaus, G.; Schuller, D.; Schumpe, A. *J. Chem. Eng. Data* **1984**, *29*, 286.
(49) Joubert-Huebner, E.; Gerdes, A.; Sievers, H. *Perfusion* **2000**, *15*, 69.
(50) *Physical properties of glycerine and its solutions*; Glycerine Producers' Association: New York, 1963.
(51) Ren, T.; Cong, L.; Wang, Y.; Tang, Y.; Tian, B.; Lin, X.; Zhang, Y.; Tang, X. *Expert Opin. Drug Delivery* **2013**, *10*, 1533.
(52) Walton, J. C. In *Encyclopedia of Radicals in Chemistry, Biology and Materials*; Chatgillaloglu, C., Studer, A., Eds.; John Wiley & Sons, Inc.: New York, 2012.
(53) Kogan, A.; Garti, N. *Adv. Colloid Interface Sci.* **2006**, *123*, 369.
(54) Battino, R. *Oxygen and ozone. IUPAC solubility data series*; Pergamon Press: Oxford, U.K., 1981; Vol. 7.
(55) Liu, K. J.; Gast, P.; Moussavi, M.; Norby, S. W.; Vahidi, N.; Walczak, T.; Wu, M.; Swartz, H. M. *Proc. Nat. Acad. Sci.* **1993**, *90*, 5438.
(56) Pandian, R. P.; Raju, N. P.; Gallucci, J. C.; Woodward, P. M.; Epstein, A. J.; Kuppusamy, P. *Chem. Mater.* **2010**, *22*, 6254.
(57) Eteshola, E.; Pandian, R. P.; Lee, S. C.; Kuppusamy, P. *Biomed. Microdevices* **2009**, *11*, 379.
(58) Rübe, A.; Hause, G.; Mäder, K.; Kohlbrecher, J. *J. Controlled Release* **2005**, *107*, 244.
(59) de Melo, N. F. S.; Grillo, R.; Guilherme, V. A.; de Araujo, D. R.; de Paula, E.; Rosa, A. H.; Fraceto, L. F. *Pharm. Res.* **2011**, *28*, 1984.
(60) Kroll, C. PhD thesis, Humboldt-Universität zu Berlin, Mathematisch-Naturwissenschaftliche Fakultät I, 1999.
(61) Rübe, A.; Mäder, K. *J. Biomed. Nanotechnol.* **2005**, *1*, 208.
(62) Kuethe, J. T. *J. Labelled Compd. Radiopharm.* **2012**, *55*, 180.
(63) Fessi, H.; Puisieux, F.; Devissaguet, J. P.; Ammoury, N.; Benita, S. *Int. J. Pharm.* **1989**, *55*, R1.

DOI: 10.1021/acs.joc.5b00918
J. Org. Chem. 2015, 80, 6754−6766